

Formation Mechanisms of the $2\text{CaO}\cdot\text{SiO}_2\text{-}3\text{CaO}\cdot\text{P}_2\text{O}_5$ Solid Solution at Hot Metal Dephosphorization Process

Fumitaka TSUKIHASHI

Professor

Department of Advanced Materials Science,
Graduate School of Frontier Sciences,
The University of Tokyo

1. Introduction

Decrease of phosphorus content in the melt at steelmaking processes is one of the important issues and thus development of hot metal dephosphorization process has been extensively conducted last three decades to meet the demand of high quality grade steels. Since dephosphorization reaction proceeds with high basic slag, at oxidizing condition, and at lower temperature, CaO based fluxes have been used due to the basic property of CaO and abundance as domestic resource with low cost. Oxygen gas or iron oxide is used as oxidizer and thus the dephosphorization flux is the FeO-CaO-SiO₂-P₂O₅ system. However, the practical flux contains large amount of solid CaO dispersed in liquid flux, because of relatively low temperature around 1573 K during hot metal pretreatment resulting low solubility of CaO into the flux. Currently large amount of CaO have been added as a flux to enhance the dissolution of solid CaO. Therefore, utilization efficiency of CaO is low and unreacted CaO remains in the slag, which increases the slag volume and prevents smooth slag recycling. Although CaF₂ was previously used to dramatically increase the solubility of CaO, the addition of CaF₂ to the flux is strictly regulated from the environmental view point. Reduction in the volume of dephosphorization slag without using CaF₂ is strongly required.

Many researches regarding the dissolution of CaO in the liquid slag have been reported. Schlitt *et al.*¹⁾ found the dissolution rate of CaO increased significantly with increasing FeO content. Dissolution rate is also affected by the additives²⁾ such as CaF₂, CaCl₂, Al₂O₃, B₂O₃, or by CaO particle size.³⁾ It is well known P₂O₅ in steelmaking slag after solidification is condensed to 2CaO·SiO₂ phase.^{4,5)} Ito *et al.*⁶⁾ and Hirosawa *et al.*⁷⁾ measured the partition of phosphorus between liquid slag and solid 2CaO·SiO₂ at hot metal pretreatment temperature. Inoue *et al.*⁵⁾ reported that the formation of CaO-SiO₂-P₂O₅ occurs within 5 s. The 2CaO·SiO₂-3CaO·P₂O₅ pseudo binary system has very wide solid solution range and also Silicocarnotite (5CaO·SiO₂·P₂O₅) and Nagelschmidite (7CaO·2SiO₂·P₂O₅) are formed at hot metal pretreatment temperature⁸⁾. Therefore, efficient hot metal dephosphorization process will be achieved with multi phase fluxes containing solid CaO if P₂O₅ in liquid slag could be condensed to 2CaO·SiO₂ phase.

The objective of this research is to elucidate the formation mechanism of the 2CaO·SiO₂-3CaO·P₂O₅ solid solution in the dephosphorization process and the following two topics are focused on, namely (1) reaction behavior between solid CaO or 2CaO·SiO₂ and FeO-CaO-SiO₂-P₂O₅ liquid, and (2) phase equilibria between solid 2CaO·SiO₂-3CaO·P₂O₅ and liquid phase for the FeO-CaO-SiO₂-

P₂O₅ system.

2. Experimental

2.1. Reaction between Solid CaO/2CaO·SiO₂ and FeO-CaO-SiO₂-P₂O₅ Slag

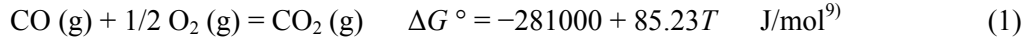
A SiC resistance furnace with a mullite reaction tube (O.D. 70 mm, I.D. 63 mm, L 1000 mm) was employed for the experiment. The slag sample was produced by mixing synthesized wüstite, calcined CaO, and reagent grade SiO₂ and 3CaO·P₂O₅. A CaO piece of 3 g was cut from a chunk of CaO (purity: 99.9 %, density: 3.3×10³ kg/m³) and used as solid CaO specimen. A 2CaO·SiO₂ piece was produced by pressing and heating a mixture of calcined CaO and reagent grade SiO₂ on molar ratio of 2:1, together with 1 mass% 3CaO·P₂O₅ to prevent the dusting of 2CaO·SiO₂ during cooling. All solid specimens were polished to obtain the plain reaction surface.

Ten grams of mixed slag sample was charged in an alumina crucible (O.D. 38 mm, I.D. 34 mm, H 45 mm), and the crucible was put inside a reaction tube heated at experimental temperature. The slag was held for one hour to ensure the equilibrium at CO-CO₂ atmosphere (CO/CO₂=100/1), or Ar atmosphere with a solid electrolytic iron piece submerged in the slag. The solid CaO or 2CaO·SiO₂ piece attached to the tip of the ceramic tube was firstly inserted in the reaction tube and held near the slag to preheat the piece for 120 s, and then dipped into the liquid slag to react. The count of reaction time started when the solid piece was dipped, and after the prescribed reaction time the solid sample was quickly taken out from the furnace and quenched in flushing Ar gas or by immersing into liquid nitrogen. Quenched sample was embedded in the polyester resin and the cross section of the interface between solid piece and slag was exposed by polishing the embedded sample and coating with 13 nm thickness Au layer. The interface was observed and the chemical composition was analyzed by SEM(JEOL JSM-6060LV) with EDS(JEOL EX-54175JMU). For the calculation of slag compositions from element compositions determined by EMS, FeO, CaO, SiO₂, P₂O₅, and Al₂O₃ oxides were assumed. The spot size of electron beam was about 2 μm.

2.2. Equilibria between Solid 2CaO·SiO₂-3CaO·P₂O₅ and Liquid Phase for the FeO-CaO-SiO₂-P₂O₅ System

A MoSi₂ resistance furnace with an alumina reaction tube (O.D. 60 mm, I.D. 50 mm, L 1000 mm) was employed for the experiment. A sample was put in a Pt crucible (O.D. 5.1 mm, I.D. 4.9 mm, H 5.0 mm). After increasing the hot zone temperature to 1923 K and changing the inside of the tube to Ar gas, a Pt crucible containing 0.1 g oxide specimen prepared by mixing FeO, CaO, SiO₂ and 3CaO·P₂O₅ was put in the hot zone by suspending with Pt wire (φ 0.5 mm). After 1 h for pre-melting, the furnace temperature decreased to 1673 K with 6 K/min and then CO-CO₂ gas (CO/CO₂=5/1) was introduced with 200 cm³/min. The sample was held for 5 h, where the oxygen partial pressure was controlled to be 9.1×10⁻¹¹ atm by Eq. (1). After the sample was equilibrated, the crucible was quickly pulled up to the top of the tube and quenched by flushing Ar gas inside the tube. The quenched sample was embedded in the polyester resin and the slag was exposed by polishing with SiC papers and diamond suspensions up to 1 μm. After coating with carbon, the sample was analyzed by SEM with

EDS as previously mentioned. Since solidification structure was observed in several samples, the area composition analysis of 300 s was applied for such samples. The EDS analyses were conducted for 5 to 30 positions for each phase to calculate the average composition.



3. Results and Discussion

3.1. Reaction between Solid CaO/2CaO·SiO₂ and Molten FeO-CaO-SiO₂-P₂O₅ Slag

(a) Reaction between CaO and slag¹⁰⁾

Figures 1(a) to (d) show the SEM images around the interface between solid CaO and 25 mass%FeO-31%CaO-33%SiO₂-11%P₂O₅ slag at 1573 K reacted for 2 to 30 s. The numbered positions in figures were analyzed by EDS to obtain the chemistry. The CaO-FeO phase was observed adjacent to solid CaO, and the CaO-SiO₂ or CaO-SiO₂-P₂O₅ phase surrounded by liquid FeO-CaO-SiO₂ with high FeO content was formed next to the CaO-FeO layer. SiO₂ content in the CaO-FeO phase was less than 5 mass% and the ratio of CaO/FeO was approximately unity. Solid CaO-SiO₂ surrounded by liquid slag was identified as 2CaO·SiO₂. CaO-SiO₂-P₂O₅ particles coexisting with FeO-CaO-SiO₂ slag contained from 1 to 10 mass% of P₂O₅, and CaO-SiO₂-P₂O₅ composition was a binary mixture of 2CaO·SiO₂ and 3CaO·P₂O₅. 2CaO·SiO₂ and 3CaO·P₂O₅ make wide solid solution region.⁸⁾ Therefore, it is considered that P₂O₅ was taken into 2CaO·SiO₂ as 3CaO·P₂O₅.

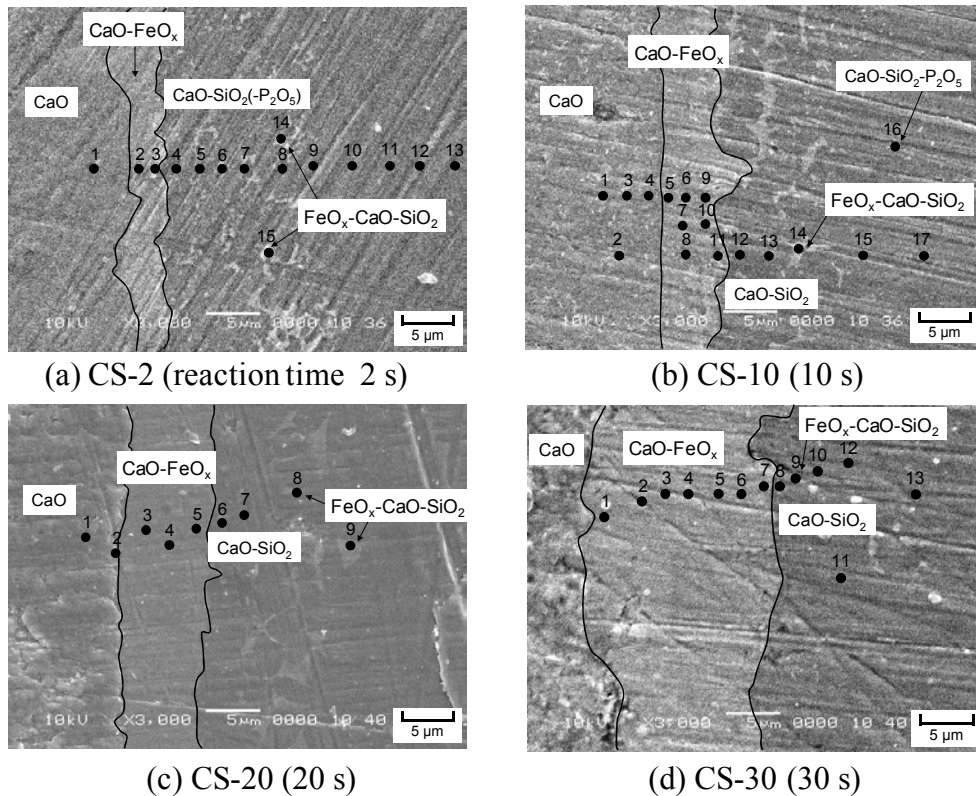


Figure 1 SEM images at the interface between solid CaO and molten slag at 1573 K.

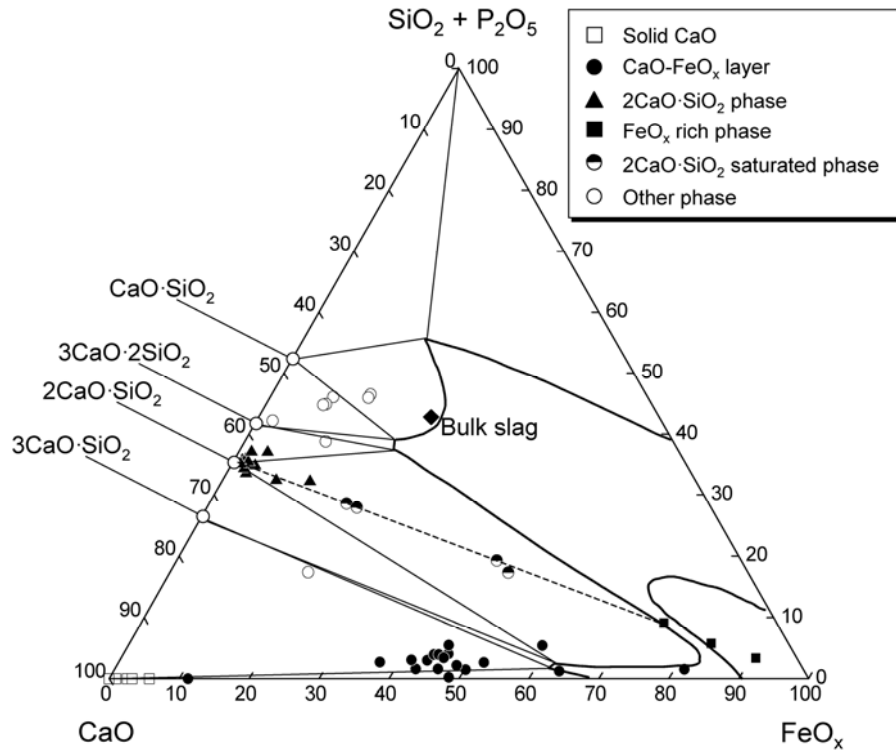


Figure 2 Projection of the chemical compositions analyzed by EDS for the FeO-CaO-(SiO₂+P₂O₅) system at 1573 K.

The compositions obtained by EDS analysis are plotted on the FeO-CaO-(SiO₂+P₂O₅) pseudo ternary diagram as shown in Fig. 2. The solid curves represent the liquidus for the FeO-CaO-SiO₂ system equilibrated with iron at 1573 K.¹¹⁾ The phases were classified into solid CaO, CaO-FeO, 2CaO·SiO₂, FeO-CaO-SiO₂ liquid with high FeO, and 2CaO·SiO₂ saturated phases. The compositions of FeO-CaO-SiO₂ liquid phase with high FeO content, coexisting with 2CaO·SiO₂, were close to the liquidus composition of 2CaO·SiO₂ saturation. Therefore, it is considered CaO content in liquid slag around solid CaO increased by CaO dissolution and local slag composition reached to the liquidus of 2CaO·SiO₂ saturation. Dissolved CaO and SiO₂ in the liquid were consumed to precipitate 2CaO·SiO₂ and the liquid phase composition changed along the liquidus resulting increase of FeO content.

The activities of FeO and CaO in the CaO-FeO phase and those in the liquid phase saturated by 2CaO·SiO₂ were estimated by using the data after Takeda and Yazawa,¹²⁾ and by the regular solution model,¹³⁾ respectively. The activity of FeO in the 2CaO·SiO₂ saturated liquid phase is higher than that in CaO-FeO phase and bulk slag. Therefore, FeO diffuses from 2CaO·SiO₂ saturated liquid phase to both the CaO-FeO phase and bulk slag. On the other hand, the activity of CaO in the CaO-FeO phase is much higher than that in other phases. Therefore, CaO diffuses from solid CaO toward bulk slag through the CaO-FeO and 2CaO·SiO₂ saturated liquid phases.

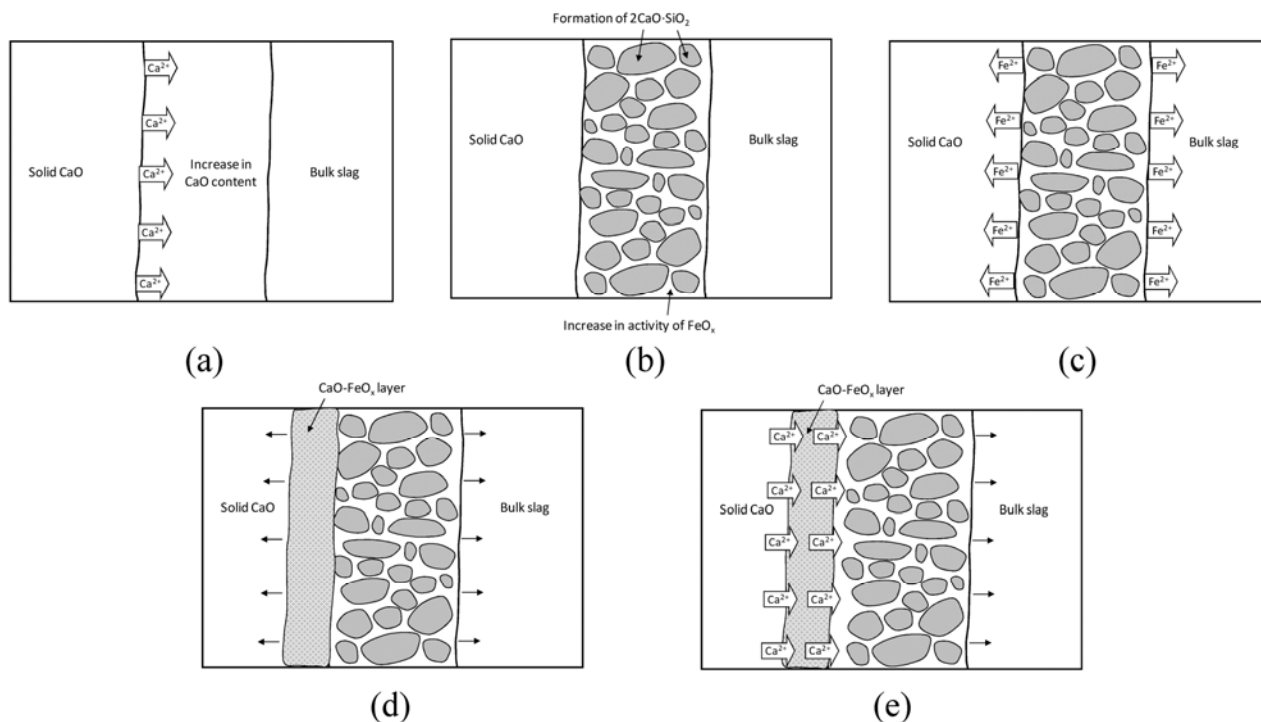


Figure 3 Schematics of reaction mechanisms.

From the above considerations, the reaction mechanisms between solid CaO and molten FeO-CaO-SiO₂-P₂O₅ slag are considered to be as follows; (1) Dissolution of CaO into the slag resulting the increase of CaO content in the melt (Fig. 3(a)), (2) Formation of 2CaO·SiO₂ from liquid slag, decrease of CaO and SiO₂ contents in the liquid, and relatively increase of FeO content (Fig. 3(b)), (3) Diffusion of FeO from FeO rich phase to both solid CaO and bulk slag (Fig. 3(c)), (4) Formation of CaO-FeO phase adjacent to solid CaO (Fig. 3(d)), and (5) Diffusion of CaO to bulk slag through formed CaO-FeO layer (Fig. 3(e)).

Figure 4 shows the relationship between P₂O₅ content in the 2CaO·SiO₂-3CaO·P₂O₅ phase and the distance from CaO-slag interface to the 2CaO·SiO₂-3CaO·P₂O₅ phase after dipping CaO in 25 mass%FeO-36%CaO-29%SiO₂-10%P₂O₅ slag at 1673 K for 2 to 10 s. P₂O₅ content increased from the CaO-slag boundary toward the bulk slag. After longer reaction time, P₂O₅ content in the 2CaO·SiO₂-3CaO·P₂O₅ phase became larger. From this result, the formation of the 2CaO·SiO₂-3CaO·P₂O₅ phase is considered to proceed through two steps; firstly, P₂O₅ in the slag is condensed as 2CaO·SiO₂-3CaO·P₂O₅ solid solution precipitated from the molten slag. Afterward, P₂O₅ is absorbed as 3CaO·P₂O₅ in the existing 2CaO·SiO₂-3CaO·P₂O₅ phase.

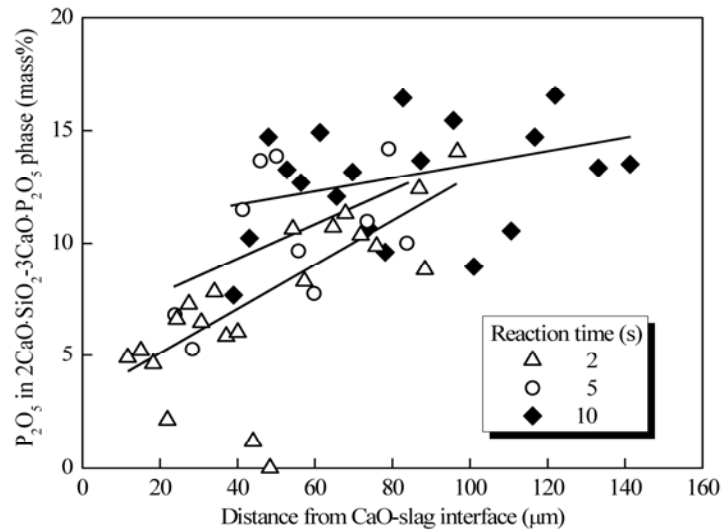


Figure 4 Relationship between P_2O_5 content in $2CaO \cdot SiO_2 - 3CaO \cdot P_2O_5$ phase and the distance from CaO-slag interface to $2CaO \cdot SiO_2 - 3CaO \cdot P_2O_5$ phase at 1673 K.

(b) Reaction between $2CaO \cdot SiO_2$ and slag¹⁴⁻¹⁷⁾

Figure 5 shows the SEM image around the interface between $2CaO \cdot SiO_2$ and 20 mass%FeO-38%CaO-32%SiO₂-10%P₂O₅ slag after the reaction for 60 s at 1673 K. The left side is the original solid $2CaO \cdot SiO_2$ and the right side is the bulk slag, though the interface is not seen clearly because the fabricated $2CaO \cdot SiO_2$ piece was porous and the slag penetrated easily inside the $2CaO \cdot SiO_2$ piece. Chemical compositions at positions represented in Fig. 5 were analyzed by EDS and plotted on the pseudo ternary diagram for the FeO-CaO-(SiO₂+P₂O₅) as shown in Fig. 6 to examine the phase distribution and relationship at the interface. In this figure, solid lines indicate the liquidus for the FeO-CaO-SiO₂ system equilibrated with solid iron at 1673 K.¹¹⁾ All phases appeared along the joint line between $2CaO \cdot SiO_2$ and the original bulk slag shown as dashed line in Fig. 6. Observed phases are categorized to solid $2CaO \cdot SiO_2$, $2CaO \cdot SiO_2$ saturated liquid slag, and the solid-liquid coexisting phase.

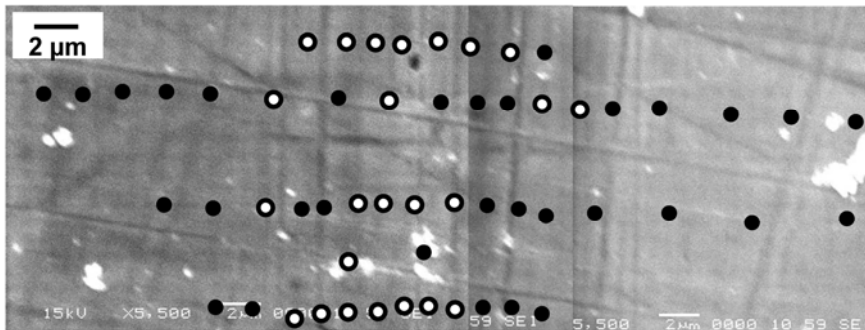


Figure 5 SEM image around the interface between solid $2CaO \cdot SiO_2$ and FeO-CaO-SiO₂-P₂O₅ slag at 1673 K.

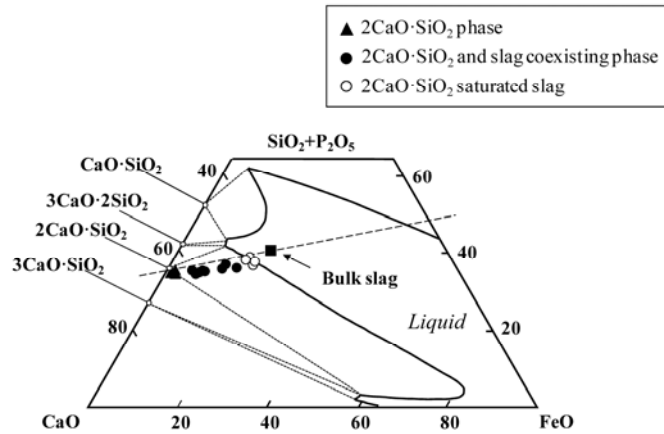


Figure 6 Phase distribution at the interface between solid $2\text{CaO}\cdot\text{SiO}_2$ and the bulk slag at 1673 K.

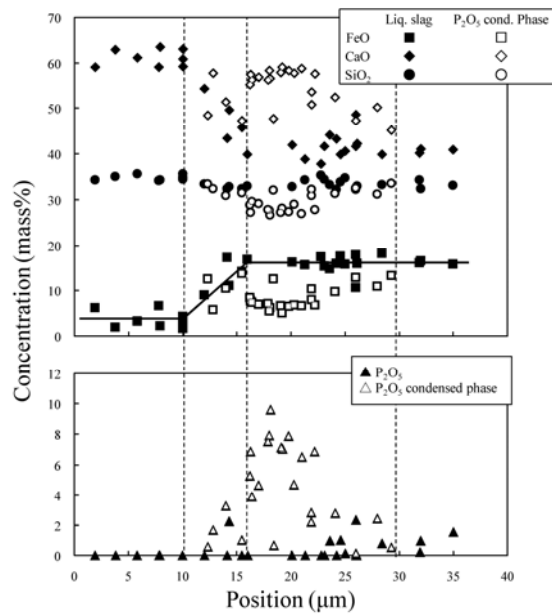


Figure 7 Concentration of oxides around the interface as a function of position after 60 s reaction at 1673 K.

The composition of each oxide was shown in Fig. 7 as a function of position. The left end of the SEM image in Fig. 5 corresponds to position 0 in Fig. 7. CaO content decreased from $2\text{CaO}\cdot\text{SiO}_2$ (left) toward bulk slag (right), while FeO content increased. SiO_2 content was almost constant. Positions in solid-liquid coexisting region in Fig. 6 with high P_2O_5 content were represented as open symbols in Fig. 7. P_2O_5 condensed phase was observed at the region where a gradient for CaO and FeO contents was seen.

The profile of FeO content showed a clear trend, and thus the region in Fig. 7 was separated by dashed line; low FeO content (left), FeO increasing region (center) and high constant FeO content (right), and these three regions correspond to solid $2\text{CaO}\cdot\text{SiO}_2$, liquid slag penetration region into $2\text{CaO}\cdot\text{SiO}_2$, and liquid slag region, respectively. Therefore, it is considered there was an initial interface between solid $2\text{CaO}\cdot\text{SiO}_2$ and liquid slag around the right side of the slag penetration layer. The P_2O_5 condensed phase, namely $2\text{CaO}\cdot\text{SiO}_2\text{-}3\text{CaO}\cdot\text{P}_2\text{O}_5$ phase, was observed around this

solid-liquid interface. It is considered the formation reaction of $2\text{CaO}\cdot\text{SiO}_2\text{-}3\text{CaO}\cdot\text{P}_2\text{O}_5$ phase is fast, because the phase was observed after the reaction for 1 s. The amount of P_2O_5 condensed phase was not large compared to that in the case of CaO dipping experiments, neither was P_2O_5 content in the phase.

The reaction mechanisms between solid $2\text{CaO}\cdot\text{SiO}_2$ and liquid $\text{FeO-CaO-SiO}_2\text{-P}_2\text{O}_5$ slag are concluded from the present results as illustrated in Fig. 8; (1)The solid $2\text{CaO}\cdot\text{SiO}_2$ dissolves into the liquid slag and also the liquid slag penetrates into the solid sample (Fig. 8(a)), (2)The rim of the solid $2\text{CaO}\cdot\text{SiO}_2$ changes into multi phase area where solid and liquid phases are coexisting, while the liquid slag turns to be saturated with $2\text{CaO}\cdot\text{SiO}_2$ (Fig. 8(b)), (3) P_2O_5 reacts with solid $2\text{CaO}\cdot\text{SiO}_2$ to form the P_2O_5 condensed phase in the multi phase region (Fig. 8(c)), (4)The multi phase region shifts towards the side of $2\text{CaO}\cdot\text{SiO}_2$ and new P_2O_5 condensed phases are formed because of continuous $2\text{CaO}\cdot\text{SiO}_2$ dissolution as well as penetration of slag into solid $2\text{CaO}\cdot\text{SiO}_2$ (Fig. 8(d)), (5)The previously formed P_2O_5 condensed phase would remain (Fig. 8(e1)), fully dissolve (Fig. 8(e2)), or partly dissolve into the slag (Fig. 8(e3)), depending on the temperature and slag composition.

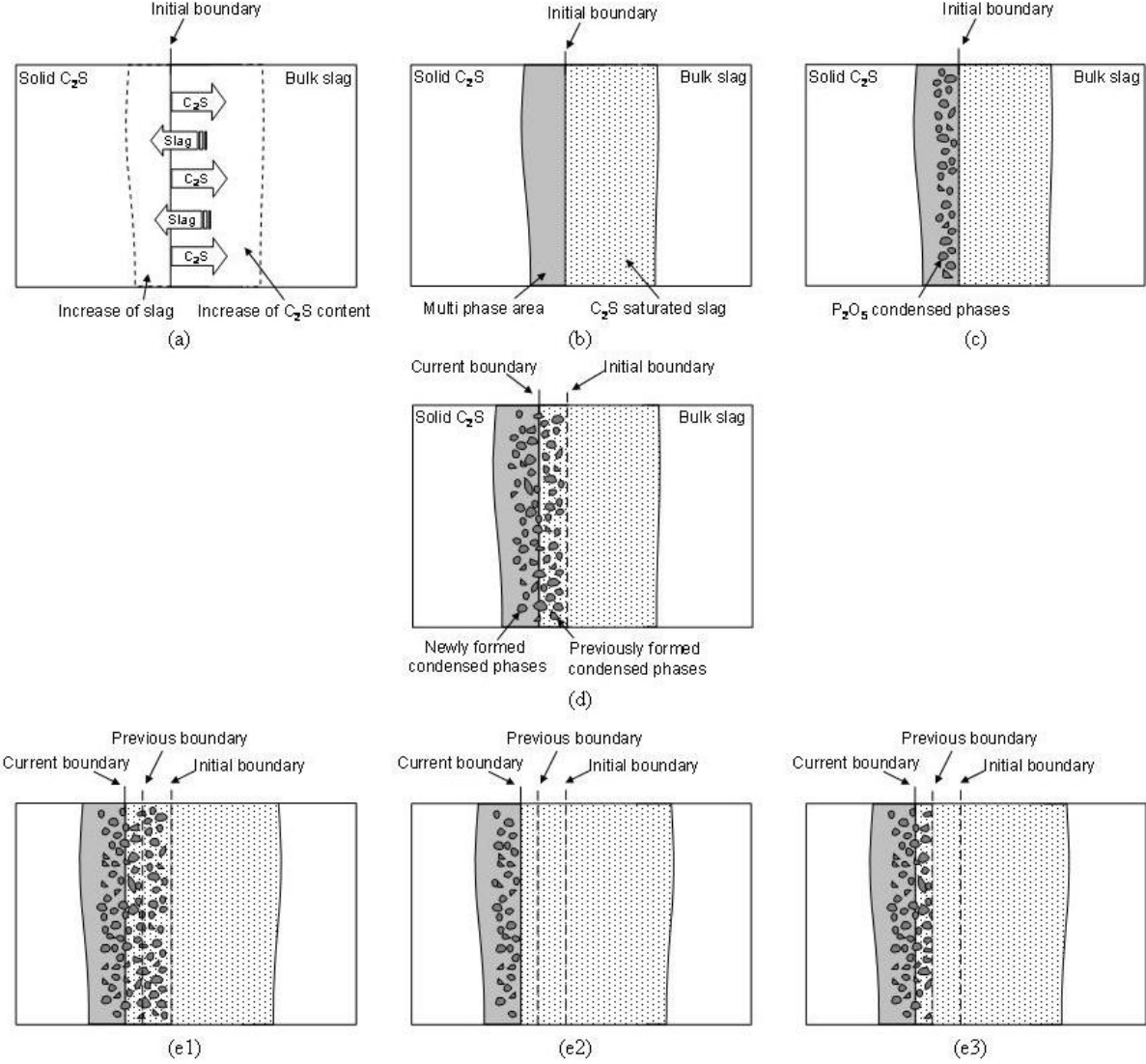


Figure 8 Reaction behavior of phosphorous at the interface between $2\text{CaO}\cdot\text{SiO}_2$ and $\text{FeO-CaO-SiO}_2\text{-P}_2\text{O}_5$ slag. C_2S is short for $2\text{CaO}\cdot\text{SiO}_2$.

3.2. Phase Equilibria between Solid $2\text{CaO}\cdot\text{SiO}_2\text{-}3\text{CaO}\cdot\text{P}_2\text{O}_5$ and Liquid Slag for the $\text{FeO-CaO-SiO}_2\text{-P}_2\text{O}_5$ System^{18,19)}

Figure 9 shows the measured liquidus at 1673 K, with the liquidus for the FeO-CaO-SiO_2 system equilibrated with solid iron.¹¹⁾ P_2O_5 was considerably concentrated in the solid phase compared to the liquid, and the large phosphorus partition ratio between solid and liquid phases was observed. The compositions of solid phases were found to be the solid solution of $2\text{CaO}\cdot\text{SiO}_2\text{-}3\text{CaO}\cdot\text{P}_2\text{O}_5$. Composition of solid phase was shifted to CaO corner from $2\text{CaO}\cdot\text{SiO}_2$ on the FeO-CaO-SiO_2 ternary phase diagram, because the increase of P_2O_5 content in the $2\text{CaO}\cdot\text{SiO}_2\text{-}3\text{CaO}\cdot\text{P}_2\text{O}_5$ phase results in the CaO/SiO_2 ratio larger than 2. Since small solubility of FeO in the solid phase was observed, it seems that small amount of CaO is substituted by FeO. P_2O_5 content in liquid phase was small. Therefore, the difference between measured and reported liquidus is due to the difference in oxygen partial pressure.

In the figure, the liquidus for the FeO-CaO-SiO_2 system with $P_{\text{O}_2} = 1.8 \times 10^{-8}$ atm at 1573 K²⁰⁾ is also shown. Similar liquidus were observed at the FeO content between 20 and 60 mass% regardless temperature or oxygen partial pressure differences. On the other hand, considerable differences were recognized at high FeO content range. The author previously clarified that the decrease in the oxygen partial pressure makes the liquid area at high FeO content region wider.²⁰⁾ Therefore, the further expansion of the liquid area was expected in the present study due to the decrease of $(\% \text{Fe}^{3+})/(\% \text{Fe}^{2+})$ ratio. However, the shrinkage of the liquid area at high FeO content region was observed oppositely. Some FeO might be reduced to form metallic Fe because the oxygen partial pressure in the present study is quite close to that of Fe-FeO equilibrium. If the reaction takes place, the formed Fe causes the overestimation of Fe content in the slag which makes the liquid area narrower than the actual.

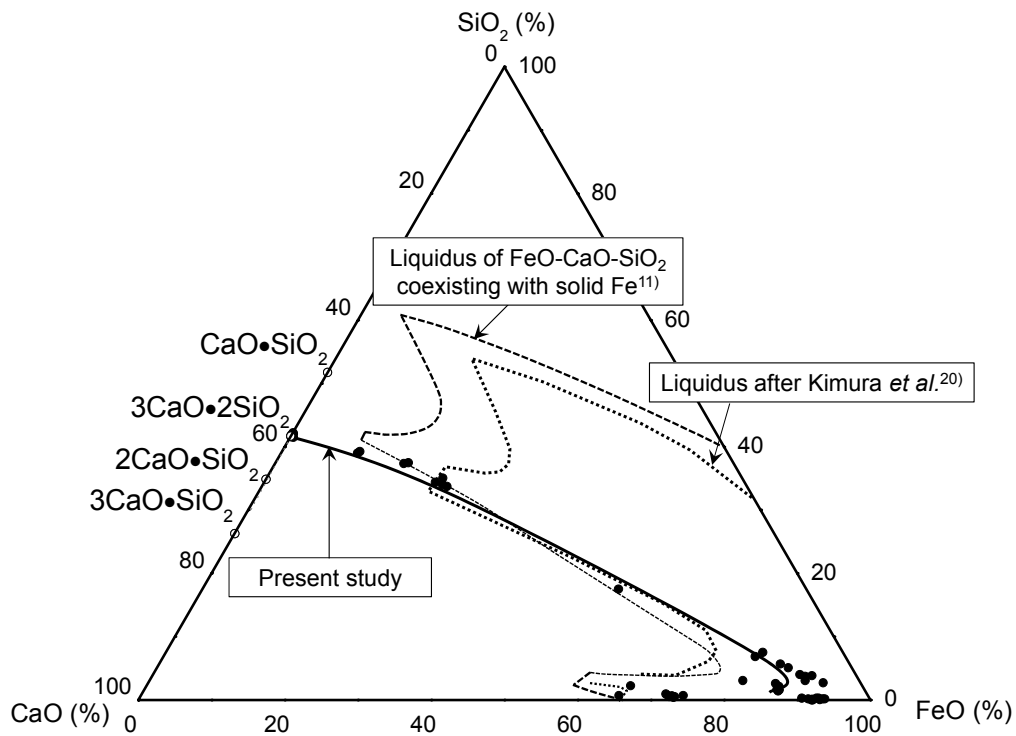


Figure 9 Measured liquidus for the FeO-CaO-SiO₂-P₂O₅ system saturated with solid 2CaO·SiO₂-3CaO·P₂O₅ at 1673 K with $P_{O_2} = 9.1 \times 10^{-11}$ atm, together with the liquidus for the FeO-CaO-SiO₂ system equilibrated with solid iron at 1673 K,¹¹⁾ and that with $P_{O_2} = 1.8 \times 10^{-8}$ atm at 1573 K.²⁰⁾

4. Conclusions

The present study focuses on the formation mechanisms of the 2CaO·SiO₂-3CaO·P₂O₅ solid solution in the FeO-CaO-SiO₂-P₂O₅ system. Firstly the reaction behavior between solid CaO/2CaO·SiO₂ and liquid FeO-CaO-SiO₂-P₂O₅ slag has been observed. Secondly, the phase equilibria between solid 2CaO·SiO₂-3CaO·P₂O₅ and liquid phase for the FeO-CaO-SiO₂-P₂O₅ system have been measured at 1673 K with $P_{O_2} = 9.1 \times 10^{-11}$ atm.

By immersing solid CaO or 2CaO·SiO₂ in the liquid slag containing P₂O₅, 2CaO·SiO₂-3CaO·P₂O₅ solid solution was formed at the interface between solid and liquid and the fast formation rate of solid solution was expected. Efficient and continuous dephosphorization reaction is possible by enhancing the condensation of P₂O₅ in solid phase and maintaining P₂O₅ content in liquid phase low. Reaction mechanisms between solid CaO/2CaO·SiO₂ and liquid slag were clarified.

Measurement of the phase equilibria proved the large phosphorus partition ratio between solid and liquid phases. The partition ratio became larger with larger FeO content.

Acknowledgment

This research was supported by JFE 21st Century Foundation for FY 2009. The author expresses his great gratitude to their support.

References

- 1) W. J. Schlitt and G. W. Healy: *Am. Ceram. Soc. Bull.*, **50** (1971), 954.
- 2) T. Hamano, M. Horibe and K. Ito: *ISIJ Int.*, **44** (2004), 263.
- 3) J. Yang, M. Kuwabara, T. Asano, A. Chuma and J. Du: *ISIJ Int.*, **47** (2007), 1401.
- 4) H. Suito, Y. Hayashida and Y. Takahashi: *Tetsu-to-Hagané*, **63** (1977), 1252.
- 5) R. Inoue and H. Suito: *ISIJ Int.*, **46** (2006), 174.
- 6) K. Ito, M. Yanagisawa and N. Sano: *Tetsu-to-Hagané*, **68** (1982), 342.
- 7) S. Hirose, K. Mori and T. Nagasaka: *CAMP-ISIJ*, **17** (2004), 868.
- 8) W. Fix, H. Heymann and R. Heinke: *J. Am. Ceram. Soc.*, **52** (1969), 346.
- 9) E. T. Turkdogan: *Physical Chemistry of High Temperature Technology*, Academic Press, New York, (1980), 7.
- 10) R. Saito, H. Matsuura, K. Nakase, X. Yang and F. Tsukihashi: *Tetsu-to-Hagané*, **95** (2009), 258.
- 11) E. F. Osborn and A. Muan: *Phase Equilibrium Diagrams of Oxide Systems*, the American Ceramic Society and the Edward Orton Jr., Columbus, Ohio, (1960), Plate 7.
- 12) Y. Takeda and A. Yazawa: *J. Min. Metall. Inst. Jpn.*, **96** (1980), 901.
- 13) S. Ban-ya: *ISIJ Int.*, **33** (1993), 2.
- 14) X. Yang, H. Matsuura and F. Tsukihashi: *Tetsu-to-Hagané*, **95** (2009), 268.
- 15) X. Yang, H. Matsuura and F. Tsukihashi: *ISIJ Int.*, **49** (2009), 1298.
- 16) X. Yang, H. Matsuura and F. Tsukihashi: *ISIJ Int.*, **50** (2010), 702.
- 17) X. Yang, H. Matsuura and F. Tsukihashi: *Mater. Trans.*, **51** (2010), 1094.
- 18) X. GaO, H. Matsuura and F. Tsukihashi: *CAMP-ISIJ*, **23** (2010), 951.
- 19) X. GaO, H. Matsuura and F. Tsukihashi: *Proc. Fourth Baosteel Biennial Academic Conference*, (2010), B12.
- 20) H. Kimura, S. Endo, K. Yajima and F. Tsukihashi: *ISIJ Int.*, **44** (2004), 2040.